microRNA-206 attenuates tumor proliferation and migration involving the downregulation of *NOTCH3* in colorectal cancer

XIAO-WEI WANG[1*], XUE-QIN XI[2*], JIAN WU[3], YI-YUAN WAN[1], HONG-XIA HUI[1] and XIU-FENG CAO[4]

[1]Department of Medical Oncology, Huai'an First People's Hospital, Nanjing Medical University, Huai'an, Jiangsu 223300; [2]Department of Clinical Laboratory, Huai'an Hospital Affiliated to Xuzhou Medical College, Huai'an, Jiangsu 223002; [3]Department of Pathology, Huai'an First People's Hospital, Nanjing Medical University, Huai'an, Jiangsu 223300; [4]Department of Surgical Oncology, Nanjing First Hospital, Nanjing Medical University, Nanjing, Jiangsu 210000, P.R. China

Received September 25, 2014; Accepted December 19, 2014

DOI: 10.3892/or.2015.3731

Abstract. Colorectal cancer (CRC) is the most common cancer diagnosed worldwide, and the development of metastases is a major cause of mortality. Accumulating evidence suggests that microRNAs are important in carcinogenesis by affecting the expression of genes that regulate cancer progression. A number of studies have shown that miR-206 is frequently downregulated in many human malignancies, including CRC, and is associated with a more malignant phenotype. Previous studies involving HeLa and C2C12 cells have validated the inhibitory mechanism of miR-206 via *NOTCH3* targeting. However, whether or not the interplay between miR-206 and *NOTCH3* also occurs in CRC is unknown. Therefore, we investigated the tumor suppressive and metastatic effects of miR-206 and its target, *NOTCH3*, in CRC. Based on the inverse association between the expression of miR-206 and NOTCH3 in CRC tissues, miR-206 mimics were transiently transfected into the SW480 (and its metastatic strain) and SW620 colon cancer cell lines. Upregulation of miR-206 inhibited cancer cell proliferation and migration, blocked the cell cycle, and activated apoptosis. The tumor suppressive capacity of miR-206 had a similar effect on CRC cells, although with a different metastatic potential, and may be explained by direct *NOTCH3* signaling inhibition and indirect cross-talk with other signaling pathways involving CDH2 and MMP-9. These results support miR-206 as a tumor suppressor in CRC and suggest a potential therapeutic target for clinical intervention.

Correspondence to: Professor Xiu-Feng Cao, Department of Surgical Oncology, Nanjing First Hospital, Nanjing Medical University, 300 Guangzhou Road, Nanjing, Jiangsu 210000, P.R. China
E-mail: cxf551101@sina.com

*Contributed equally

Key words: colorectal cancer, miR-206, *NOTCH3*, proliferation, migration

Introduction

Colorectal cancer (CRC) is the third and second most common cancer diagnosed in males and females, respectively, with >1.2 million new cancer cases diagnosed and >0.6 million mortalities annually (1). Although patients diagnosed with localized disease have a 5-year survival rate as high as 90.3%, this rate significantly decreases to 12.5% in patients with distant metastasis (2). Mutation, phenotypic drift, epithelial-mesenchymal transition (EMT), collective migration, resistance to apoptosis and anoikis, vascularization, and lymphangiogenesis are among the known mechanisms of metastasis (3). Thus, mechanism-based targeted therapies been on the increase and are thought to have high efficacy that inhibits a target, while having relatively fewer off-target effects and thus less non-specific toxicity. By contrast, a targeted therapeutic agent that inhibits a key pathway in a cancer cell may not completely eradicate the entire tumor, allowing residual heterogenic cancer cells to survive, followed by almost inevitable relapses (4). Accumulating evidence suggests that microRNAs (miRNAs) are important in carcinogenesis by affecting the expression of genes that regulate cancer progression (5). When specific miRNAs involved in the process of metastasis are identified, therapeutic strategies can be developed to silence oncogenes or upregulate tumor-suppressor genes.

microRNA-206, unlike other myomiR family members, has been consistently identified based on Northern blot, microarray, RNase protection assays, and RT-PCR to be highly expressed in skeletal muscle (6). Recently, the findings of a number of studies have shown that miR-206 is frequently downregulated in many human malignancies, including breast cancer (7), rhabdomyosarcoma (8), renal (9), lung (10), laryngeal (11), endometrioid (12), colorectal (13), gastric cancers (14) and melanoma (15), suggesting that miR-206 is associated with a more malignant phenotype (10,13,16). Furthermore, miR-206, in combination with miR-21, -135a, -335 and let-7a, can be used as a prognostic panel for detecting the presence of metastasis in human CRCs, with a specificity and sensitivity of 87 and 76%, respectively (13). Oncogenes, including *CCND1* (15), *ESR1* (17), *MET* (18), and *NOTCH3* (19), have been identified and confirmed to be targets of miR-206, suggesting

that miR-206 has a tumor-suppressor role in CRC. Of these targets, *NOTCH3*, identified as the third mammalian Notch receptor and expressed in proliferating neuroepithelium (20), has been reported to be frequently expressed in human CRC tissues and has been shown to play a role in the modulation of CRC cell proliferation and tumorigenic potential in xenograft models (21). Previous studies have validated the inhibitory mechanism of miR-206 through its seed match region binding to the *NOTCH3* 3' untranslated region, although in the context of HeLa and C2C12 cells (19,22). However, whether the interplay between miR-206 and *NOTCH3* occurring in CRC is important is unknown.

In the present study, the expression of miR-206 and *NOTCH3* in CRC tissues and cell lines was analyzed. Based on an inverse association between the expression of this molecular pair, miR-206 mimics were transiently transfected into the SW480 (and the metastatic strain) and SW620 colon cancer cell lines. The results showed that upregulation of miR-206 inhibited cancer cell proliferation and migration, blocked the cell cycle, and activated apoptosis, even in SW620 cells, exhibiting a more aggressive property and involving NOTCH3 signaling, EMT, and extracellular matrix degradation. Therefore, our results confirmed miR-206 as a tumor suppressor in CRC and suggested a potential therapeutic target for clinical intervention.

Materials and methods

Patients and tissue samples. Approval from the Institutional Review Board of Huai'an First People's Hospital was obtained for the present study. A total of 49 sequential patients who underwent surgery for the first manifestation of CRC were included. Patients who underwent preoperative radiation or chemotherapy were not included in this study. Tumors were staged according to the AJCC Cancer Staging Manual (6th edition). The primary tumors, but not the metastatic lesions, were fixed in 10% formalin, embedded in paraffin and cut (5-8 μm) for routine histopathology examination by the Department of Pathology (Huai'an First People's Hospital, China). The tissue samples were snap-frozen and stored at -80˚C for RNA and protein extraction.

Immunohistochemistry. Tissue sections were deparaffinized and rehydrated, and then incubated for heat-induced antigen retrieval in 0.01 M citrate buffer (pH 6.0) at 100˚C for 10 min. After cooling to room temperature, 0.6% H_2O_2/80% methanol was applied to the sections for 10 min at room temperature to eliminate endogenous peroxidation. After washing with D-PBS, the sections were blocked with 10% bovine serum albumin and 0.2% Triton X-100 in D-PBS at room temperature for 30 min prior to incubation with anti-NOTCH3 rabbit polyclonal antibody (AB61043a, Sangon, Shanghai, China) diluted 100-fold at 4˚C overnight. After washing with PBS-T, the sections were applied with the Polink-1 HRP DAB detection system (ZSGB-BIO, Beijing, China) for color development. After the reaction was stopped by washing, the sections were counterstained with hematoxylin, dehydrated with alcohol, mounted with neutral balsam and imaged on a BX51 microscope with an E-620 digital camera (Olympus, Tokyo, Japan).

In situ hybridization. After rehydration in water, the sections proceeded to hybridization using an Enhanced Sensitive ISH detection kit (Boster, Wuhan, China) according to the manufacturer's instructions. Briefly, the sections were treated with pepsin at 37˚C for 10 min, washed with 0.5 M TBS and DEPC-treated water, pre-hybridized at 40˚C for 1 h, and hybridized with 100 nM 5'-digoxigenin (DIG)-labeled LNA™ probe against hsa-miR-206 at 50˚C for 8 h. After hybridization, the slides were washed with 2X, 0.5X and 0.2X SSC, sequentially. The slides were then blocked for 30 min at 37˚C, and incubated with biotinylated anti-DIG antibody at 37˚C for 2 h. After 0.5 M TBS washing, alkaline phosphatase (AP)-conjugated streptavidin was applied to the section for 1 h at room temperature. Immediately after washing the slides, AP substrate containing 0.2 mM levamisol was applied to the sections protected from light at 30˚C for 2 h. When the desired intensity of chromogenic reaction was reached, the slides were washed with water, mounted in aqueous medium and imaged on a BX51 microscope with an E-620 digital camera (Olympus, Tokyo, Japan).

Cell lines, in vitro culture and transfection. The SW480 and SW620 human colon cancer cell lines were obtained from the Shanghai Institutes of Biological Sciences (Shanghai, China). The cells were cultured in Leibovitz's L-15 medium (Gibco, Grand Island, NY, USA) supplemented with 10% HyClone® fetal bovine serum (Thermo Scientific, Beijing, China). The cells were maintained at 37˚C and 5% CO_2 in a humidified incubator to near confluence and were deprived of serum for 16 h prior to use in the experiments. Experimental data were obtained from cells passaged between 3 and 10.

For transient transfection, the cells were first cultured to reach 50-75% confluence and transfected with 100 nM miR-206 mimic or scrambled negative control (GenePharma, Shanghai, China) with Lipofectamine 2000 (Life Technologies, Carlsbad, CA, USA) according to the manufacturer's instructions.

Total RNA extraction and reverse transcription-quantitative PCR (RT-qPCR). Tissue samples or cultured cells were homogenized in TRIzol® reagent (Life Technologies). Total RNA extraction was performed as described in the manufacturer's instructions with one modification, i.e., that isopropanol precipitation was proceeded at -20˚C overnight instead of at room temperature for 10 min (23). RNA concentration was measured by the NanoDrop 1000 UV/Vis spectrophotometer (Thermo Scientific, Wilmington, DE, USA).

Prior to reverse transcription, RNAs were treated with DNase I (NEB, Beijing, China) according to the manufacturer's instructions. For amplification of *ACTB*, *NOTCH3*, *JAG1*, *HEY1*, *CDH2*, *MMP9* mRNA and RNU6-1, cDNA was generated using the ReverTra Ace-α-® Reverse Transcription kit (Toyobo, Japan) with random $(dN)_9$ primer. According to the manufacturer's instructions, the reaction was performed on 250 ng of total RNA in 10 μl total volume as follows: 30˚C for 10 min, 42˚C for 30 min, 99˚C for 5 min and stored at -20˚C. Concerning miR-206, primers for reverse transcription and qPCR were designed as previously described (24). A pulsed gene-specific RT reaction (46) in 10 μl total volume containing 250 ng RNA and 4 nM stem-loop primer [5'-CTCAACTGGTGTCGTGGAGTCGGCAATTCAGTTG

AGCCACACAC-3', (24)] was applied as follows: 16˚C for 30 min, followed by 60 cycles at 20˚C for 30 sec, 42˚C for 30 sec and 50˚C for 1 sec, then 99˚C for 5 min and stored at -20˚C.

DyNAmo™ ColorFlash SYBR-Green® qPCR kit (Thermo Scientific, Espoo, Finland) was used with a modified version relating to the volumes of reagents and cDNA in 10 μl total volume: 5 μl of 2X master mix, 1 μl RT product, and 180 nM forward and reverse primer pairs. The primers used in the qPCR were: *ACTB* (001101.3), forward, 5'-CACGAAACT ACCTTCAACTCC-3' and reverse, 5'-CATACTCCTGCT TGCTGATC-3'; *NOTCH3* (008716.2) forward, 5'-ACAGAC TGGATGGACACAGAG-3' and reverse, 5'-GATGTCAGC AGCAACCAGATG-3'; *JAG1* (000214.2) forward, 5'-TGTCGG TCTTCCAGTCTCC-3' and reverse, 5'-CACTGCAAATGTG CTCCGTAG-3'; *HEY1* (012258.3) forward, 5'-CATACGGC AGGAGGGAAAGG-3' and reverse, 5'-AACTCGAAGCGGG TCAGAGG-3'; *CDH2* (001792.3) forward, 5'-AGTCAACTG CAACCGTGTCT-3' and reverse, 5'-AGCGTTCCTGTTCC ACTCAT-3'; *MMP-9* (004994.2) forward, 5'-TTCTACGGCCA CTACTGTGC-3' and reverse, 5'-AGAATCGCCAGTACTTCC CATC-3'; RNU6-1 (004394.1) forward, 5'-GCAGCACATATAC TAAAATTGGAACGA-3' and reverse, 5'-AATATGGAACGC TTCACGAATTTGC-3'; and miR-206 (MIMAT0000239) forward, 5'-AGCTCGATTAAGGTGGAATGTAAGGAAGT-3' and reverse, 5'-CTCAACTGGTGTCGTGGAGTCGG-3'. Three-step qPCR for *ACTB*, *NOTCH3*, *JAG1*, *HEY1*, *CDH2* and *MMP-9* cDNA was performed as follows: 95˚C for 7 min; 40 cycles of denaturation at 95˚C for 20 sec, annealing at 60˚C for 20 sec, and extension at 72˚C for 20 sec. Two-step qPCR for RNU6-1 and miR-206 was performed as follows: 95˚C for 7 min; 40 cycles of denaturation at 95˚C for 10 sec and extension (RNU6-1 at 68˚C, miR-206 at 59˚C) for 30 sec.

RT-qPCR reactions, including RT-minus controls and no-template controls, were run in triplicate on an CFX™ 96 real-time PCR detection system (Bio-Rad, Hercules, CA, USA). The quantification cycle (Cq) was defined as the fractional cycle number at which fluorescence passes the fixed threshold determined by CFX Manager™ software ver. 1.6 (Bio-Rad). The expression level of mRNA and miRNA was calculated by the ΔCt method (25) using *ACTB* and RNU6-1, respectively, as a reference.

Western blotting. Following removal of the RNA aqueous phase from TRIzol® the remaining phenol-chloroform layer was used for protein isolation according to the manufacturer's instructions. Proteins were dissolved in 0.5% SDS/3 M urea, quantified by the BCA assay kit (CWBIO, China), and mixed with 5X SDS-PAGE sample buffer (10% SDS/5% 2-mercaptoethanol). After the samples were denatured at 95˚C for 5 min, 30 μg proteins per lane were separated by 10% SDS-PAGE and transferred to Immobilon®-P membranes (Millipore, Billerica, MA, USA). The membranes were blocked in D-PBS/0.05% Tween-20 (PBST) containing 5% defatted milk for 1 h at room temperature. The blocked membranes were then probed with anti-ACTB rabbit polyclonal antibody (Proteintech, Chicago, IL, USA), diluted at 2,000-fold; anti-NOTCH3 rabbit polyclonal antibody (Sangon, China), diluted at 250-fold; or anti-Caspase-3 rabbit monoclonal antibody (Cell Signaling Technology, Boston, MA, USA) at 4˚C overnight. After washing with PBST, the membranes were then incubated with HRP-conjugated goat anti-rabbit IgG antibody (Boster, China), diluted at 4,000-fold for 1 h at room temperature. After washing with PBST, the immunolabeling proteins were reacted with chemiluminescent HRP substrate (Millipore) and visualized by ChemiDoc™ XRS systems (Bio-Rad).

Cell proliferation and apoptosis assay. For the proliferation assay, the transfected cells were seeded in a flat-bottom 96-well plate at $1x10^4$/well. After maintaining in serum-free medium for 16 h, the cells were recovered to the culture medium followed by the addition of 20 μl/well of [3-(4,5-dimethylthiazol-2-yl) 2,5 diphenyl tetrazolium bromide)] (MTT) solution (5 mg/ml in PBS) for 4 h at 37˚C. The reaction was terminated by adding 200 μl dimethyl sulfoxide to each well, followed by gentle agitation for 20 min. The absorbance of each well was then measured at 490 nm using an Elx808 microplate reader (BioTek, Winooski, VT, USA).

At 36 h post-transfection, cells ($5x10^5$) were resuspended and stained using an Annexin V-FITC Apoptosis detection kit (BioBox, Nanjing, China), and then detected on a FACSCalibur flow cytometer (BD Biosciences, San Jose, CA, USA). The apoptotic cell level was calculated by dividing FITC-stained only cells to gated cells.

Cell cycle analysis. The cells seeded in 6-well plates at $1x10^6$cells/well were cultured and transfected as mentioned above. Following serum starvation for 16 h, the cells were digested with trypsin and neutralized with Leibovitz's L-15 medium. Cell cycle analysis was performed using a CycleTest™ Plus DNA reagent kit (BD Biosciences). Each sample was analyzed on a FACSCalibur flow cytometer (BD Biosciences). The cell subpopulations in G_0/G_1, S and G_2/M phases were calculated based on differences of DNA content.

Wound-healing assay. The cells seeded at $5x10^5$ cells/well were cultured overnight in 6-well plates. The following day, 100 nM miR-206 mimic or negative control was transfected using Lipofectamine 2000. Untransfected cells were cultured in medium as blanks. After 36 h, transfected cells were grown to confluence and wounded by dragging a 0.2-ml pipette tip through the monolayer. The cells were washed using pre-warmed PBS to remove cell debris and allowed to migrate for 24 h. The rate of wound closure was expressed as a percentage of the initial scraped gap.

Cell migration assay. Cells were seeded, cultured and transfected as described above. At 36 h post-transfection, the cells collected and resuspended in Leibovitz's L-15 medium were placed in the upper compartment at $1x10^5$/100 μl. After 10 h of incubation, the cells on the top of the membrane were removed by swiping with a damp cotton swab. The membrane was fixed with 4% paraformaldehyde for 30 min and stained with 0.1% crystal violet for 15 min. The cells on the underside of the membrane were counted using a light microscope. For each triplicate, the number of cells in 10 fields (x200 magnification) was determined, and the counts were averaged.

Statistical analysis. Data were presented as mean ± SD. A Shapiro-Wilk normality test was used to evaluate the distribution

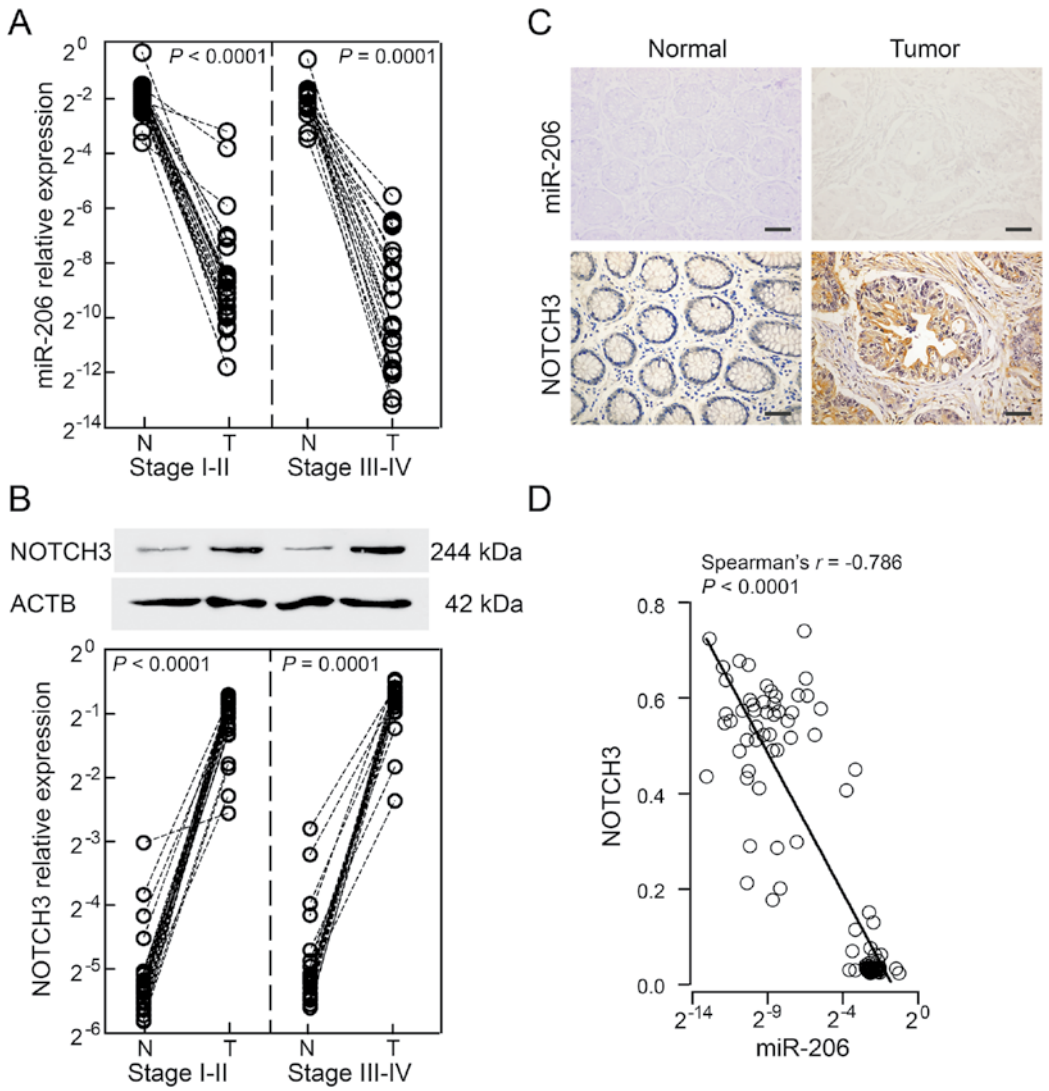

Figure 1. miR-206 expression is opposite to NOTCH3 in primary colorectal cancers. (A) The levels of miR-206 were significantly lower in tumors (T) than in normal tissues (N) of patients with Stage I-II (n=28, P<0.0001) and Stage III-IV (n=21, P=0.0001). (B) The levels of NOTCH3 protein were significantly higher in tumors (T) than in normal tissues (N) of patients with Stage I-II (n=28, P<0.0001) and Stage III-IV (n=21, P=0.0001). (C) The tissue sections were examined for miR-206 by *in situ* hybridization and NOTCH3 by immunohistochemistry. Scale bars, 50 μm. (D) miR-206 expression in the 49 colorectal patients was reverse to the NOTCH3 protein expression (Spearman's r =-0.786, P<0.0001). The levels of miR-206 were quantified by RT-qPCR and normalized to RNU6-1. The relative levels of NOTCH3 were determined by western blotting and expressed as the ratio to ACTB.

of quantitative observations. Skew distributional data expressed as median (interquartile range) were analyzed using non-parametric tests. The Wilcoxon matched-pairs signed-rank test was used to compare between tumors and matched adjacent normal tissues. A comparison between tissue samples with different stage was analyzed with the Mann-Whitney test. The correlation between miR-206 and NOTCH3 protein expression was analyzed using Spearman's rank correlation test. The *in vitro* cell experiment was repeated at ≥3 times. Two-factor analysis of variance was performed using two-way ANOVA. Data were analyzed using Stata/SE version 11.2 (StataCorp, TX, USA) and plotted in Prism® ver. 5 (GraphPad, College Station, TX, USA). P<0.05 was considered statistically significant.

Results

microRNA-206 expression is opposite to NOTCH3 in primary CRCs. According to the occurrence of metastasis, patients were enrolled in the following categories: stage I and II with non-metastatic disease (n=28); and stage III and IV with metastatic disease (n=21). Only primary tumors and matched adjacent normal tissues, but not the metastatic lesions, were analyzed in the present study. A significant difference was noted in the miR-206 expression of patients with stage I-II or stage III-IV disease between tumors and normal tissues (stage I-II: P<0.0001; stage III-IV: P=0.0001; Fig. 1A), while there were no obvious differences between stage I-II and stage III-IV patients in normal tissues or tumors (normal tissues, P=0.4057; tumors, P=0.2577). By contrast, *NOTCH3* protein was expressed in opposition to miR-206, and was significantly upregulated in tumors and minimally detected in normal tissues (stage I-II, P<0.0001; stage III-IV, P=0.0001; Fig. 1B). However, patients with advanced stages had a higher level of NOTCH3 in tumors and normal tissues (normal tissues, P=0.0306; tumors, P=0.0068). Based on these data, we further examined tissue distributions by ISH and

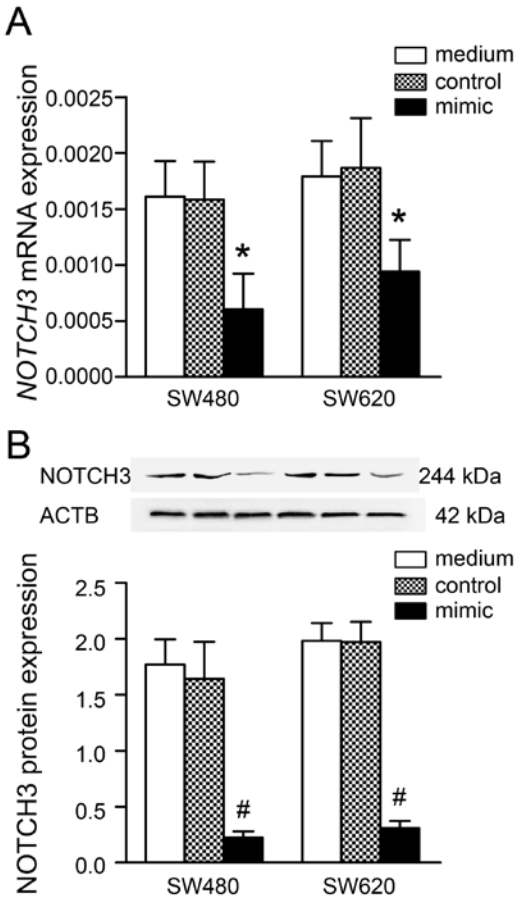

Figure 2. Upregulation of miR-206 alters *NOTCH3* expressions in colon cancer cells. Following transfection of cells with scramble normal control or miR-206 mimic (100 nM), (A) *NOTCH3* mRNA and (B) protein levels were significantly reduced in SW480 and SW620 cells. Data are shown as mean ± SD of triplicate determinations. *P<0.05 vs. medium, #P<0.001 vs. medium.

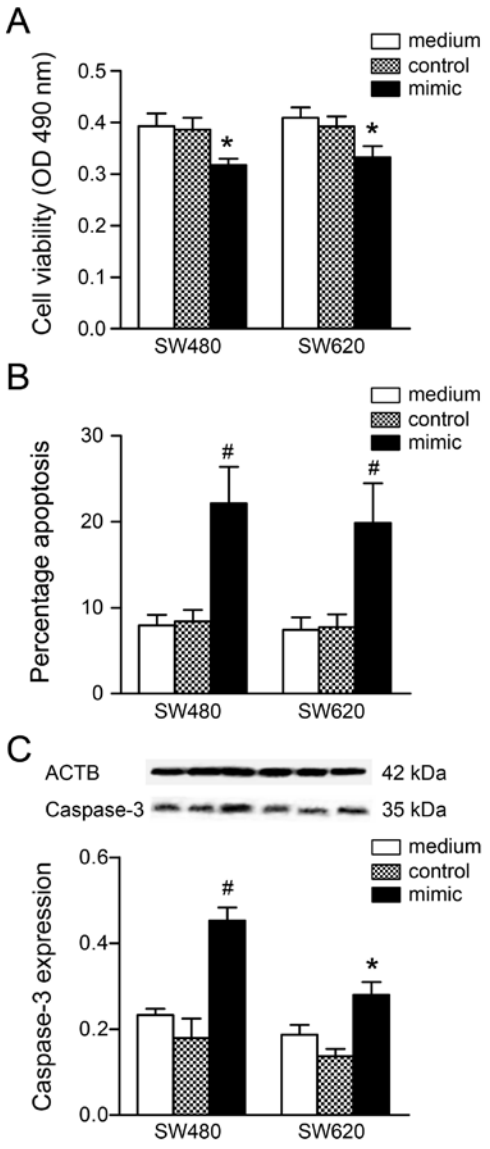

Figure 3. miR-206 inhibits cancer cell proliferation and activates apoptosis. Following transfection of cells with scramble normal control or miR-206 mimic (100 nM). (A) The cell viability measured by MTT assay was significantly reduced. (B) Apoptotic cells measured by flow cytometry. (C) Caspase-3 expression measured by western blotting was significantly increased. Data are shown as mean ± SD of triplicate determinations. *P<0.01 vs. medium, #P<0.001 vs. medium.

immunohistochemistry, respectively. microRNA-206 expression was weak-to-moderate in normal mucosa, but was absent in tumor tissues. By comparison, NOTCH3 was predominantly localized in the cytoplasm and nucleus of tumor cells with strong staining, but was rarely visible in normal mucosa (Fig. 1C). Apparently, there was an inverse association between miR-206 levels and NOTCH3 expression among the 49 CRC patients (Spearman's rho =-0.786, P<0.0001; Fig. 1D).

Upregulation of miR-206 alters NOTCH3 expression in colon cancer cells. A previous study had identified *NOTCH3* as a target of miR-206, resulting in apoptosis and migration in HeLa cells (19). To investigate the effect of miR-206 targeting *NOTCH3* in CRC, we introduced a colon cancer cell line (SW480) and a metastatic strain (SW620) for subsequent experiments. Following transfection of cells with miR-206 mimic (100 nM), *NOTCH3* mRNA and protein levels were significantly reduced in SW480 (mRNA, P<0.05; protein, P<0.001) and SW620 (mRNA, P<0.05; protein, P<0.001), which compared to the medium group (Fig. 2). As expected, treatment with scrambled negative control under the same conditions had little effect on *NOTCH3* mRNA and protein expression in the two cell lines (all tests, P>0.05). Repression of *NOTCH3* expression by miR-206 was more notable on protein translation than mRNA transcription. These findings suggested an inverse association between miR-206 and NOTCH3 expression in CRC.

miR-206 inhibits cancer cell proliferation and migration, and activates apoptosis. In view of the aforementioned data, recovery of miR-206 levels attenuated NOTCH3 protein expression, making miR-206 a potential target for therapeutic intervention. Thus, the effects of miR-206 on cell growth behavior require elucidation. Based on the MTT assay, cell viability following transfection with a miR-206 mimic (100 nM) was significantly reduced when compared to the medium group (SW480, P<0.01; SW620, P<0.01; Fig. 3A). Further examination of the cell cycle (Table I) showed that the percentage of transfected cells in the G_0/G_1 phase (SW480, P<0.01; SW620, P<0.01) was significantly increased, accompanied by a reduction in the S (SW480, P<0.05; SW620, P<0.05)

Table I. Effect of miR-206 on the cell cycle of colon cancer cells.

	SW480			SW620		
Phase	Medium	Control	Mimic	Medium	Control	Mimic
G_0/G_1	70.79±1.82	71.31±1.74	77.53±2.32[b]	69.60±2.09	70.79±1.90	76.00±1.98[b]
S	24.49±2.39	24.25±2.42	19.42±2.94[a]	25.40±1.48	24.41±1.39	20.83±1.24[a]
G_2/M	4.72±0.60	4.44±0.85	3.06±0.63[a]	5.00±0.84	4.80±0.90	3.17±0.90[a]

Cells seeded in six-well plate at $1x10^6$/well were cultured and transfected with scrambled negative control or miR-206 mimic (100 nM). The cell cycle distribution was detected by flow cytometry and the proportions of cells within G_0/G_1, S, G_2/M phases were determined. Data are shown as mean ± SD of triplicate determinations. [a]P<0.05 vs. medium, [b]P<0.01 vs. medium.

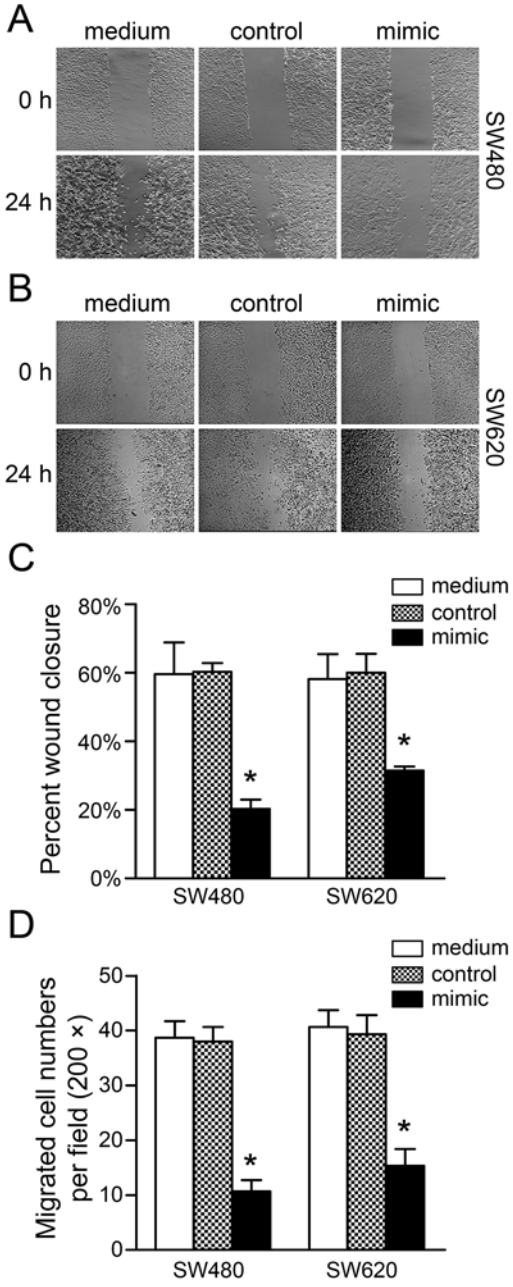

Figure 4. miR-206 reduces cancer cell migration. Following transfection with scrambled normal control or miR-206 mimic (100 nM), the cell migration was significantly decreased in the (A-C) wound healing assay or (D) Boyden chamber assay. Data are shown as mean ± SD of triplicate determinations. *P<0.001 vs. medium.

and G_2/M (SW480, P<0.05; SW620, P<0.05) phases in the two cell lines compared to the medium group. The cell cycle data obtained were consistent with the proliferation results. In addition, miR-206 mimic transfection increased the apoptotic cell number (SW480, P<0.001; SW620, P<0.001; Fig. 3B) and upregulated caspase-3 content (SW480, P<0.001; SW620, P<0.01; Fig. 3C) in the two cell lines.

To determine whether miR-206 affects migration in CRC, the wound-healing and Boyden chamber assays were used to perform cell motility measurements. Cells transfected with miR-206 mimic presented a significant reduction in the percentage of wound closure in SW480 and SW620 cells compared to the medium group (SW480, P<0.001; SW620, P<0.001; Fig. 4A-C). Similar decreases in cell migration in the two cell lines transfected with miR-206 mimic were also observed using the Boyden chamber assay compared to the medium group (SW480, P<0.001; SW620, P<0.001; Fig. 4D).

microRNA-206 affects NOTCH targets and metastasis-associated genes. We determined whether NOTCH transcriptional targets and metastasis-associated genes alter their expression following miR-206 mimic transfection. As shown in Fig. 5, the mRNA levels of two NOTCH transcriptional targets (*JAG1* and *HEY1*) and two metastasis-associated genes (*CDH2* and *MMP9*) were significantly downregulated 24 h post-transfection with miR-206 mimic in SW480 and SW620 cells. However, the basal expression of these genes, with the exception of MMP-9, had a higher level in SW620 cells, which may be relevant to its more aggressive property than SW480 cells.

Discussion

Accumulating studies acknowledge that miR-206 is a tumor suppressor that is downregulated in various tumors (7-13,15,26) and is involved in cancer metastasis (13,27). *NOTCH3*, a verified target of miR-206 (19), has also been reported to be frequently expressed in human CRC samples, and has a capacity in the modulation of CRC cell proliferation and tumorigenic potential in xenograft models (21). Therefore, we investigated the tumor suppressive and metastatic effects of miR-206 and its target (*NOTCH3*) in CRC. First, we evaluated the expression in two CRC cohorts grouped by the onset of metastasis. An inverse association between the expression of this molecular pair among the total CRC patients supported

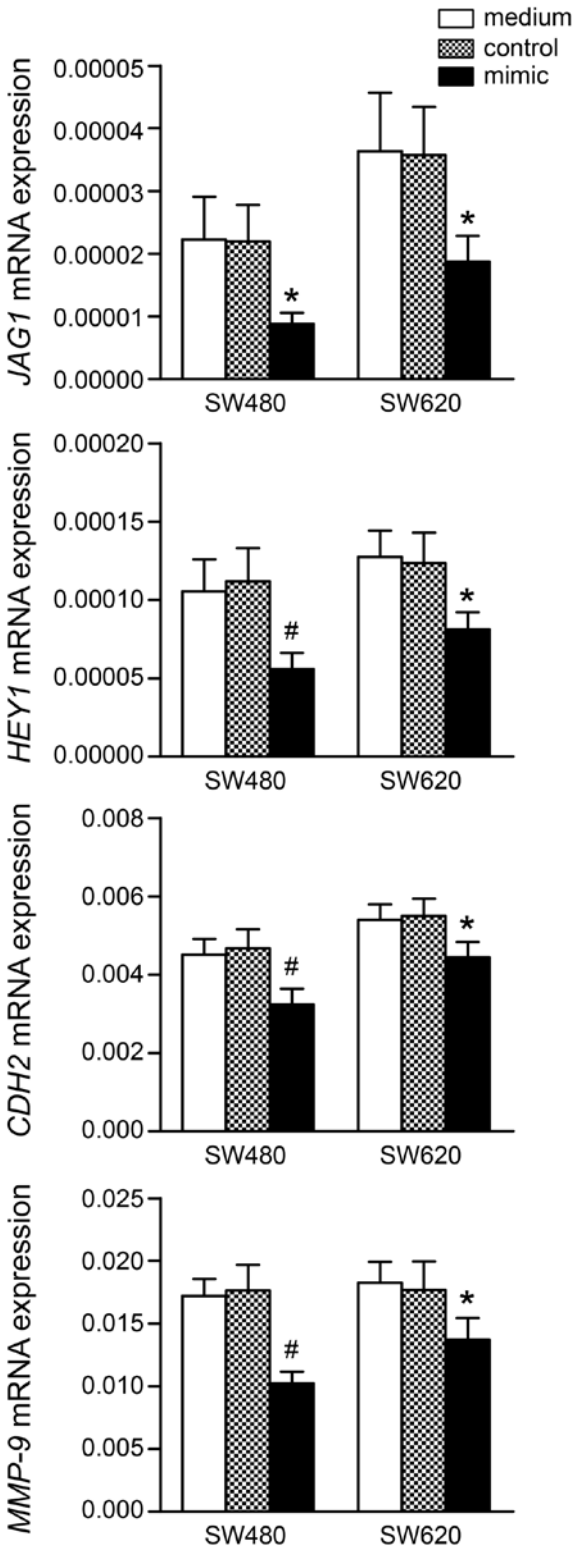

Figure 5. miR-206 affects *NOTCH* targets and metastasis-associated genes. Following cell transfection with scrambled normal control or miR-206 mimic (100 nM), the mRNA levels of *JAG1*, *HEY1*, *CDH2* and *MMP-9* were detected by RT-qPCR. Data are shown as mean ± SD of triplicate determinations. *P<0.05 vs. medium, #P<0.01 vs. medium.

the negative regulation of miR-206 targeting *NOTCH3*. miR-206 levels were further reduced with CRC progression. However, the two CRC cohorts did not differ in tumor tissue or normal mucosal miR-206 expression. This finding invalidates miR-206 as a prognostic marker used independently for metastasis, as it was combined into a 5-miR panel for predicting metastasis (13).

In CRC tissues, miR-206 was expressed at an extremely low level and was scarcely probed by ISH. Even in normal mucosa, miR-206 expression was minimal compared to tissue-specific expression in skeletal muscle. It is plausible that miR-206 is not identified in high-throughput profiling due to its low abundance in intestinal tissue (28-30). This low-abundance miRNA may regulate key components, the expression of which is markedly restricted under normal circumstances. As one such component, NOTCH3 was shown to have less expression in normal mucosa and overexpression in CRC tissue in the present study, which coincided with findings of other studies (21,31). In addition, only one mutation of the *NOTCH3* gene was detected in 48 CRC patients (32), suggesting the gene mutation may not be important in tumorigenesis. A deficiency in miR-206 in CRC may in turn make *NOTCH3*, one of its targets, lose control with intensified upregulation. A high NOTCH3 expression has been shown to be strongly correlated with metastasis in CRC (31), and may be an independent prognostic factor for hepatocellular carcinoma as well (33). Compared to a decrease of the overexpressed NOTCH3 by introducing an exogenic antagonist, rescuing the reduced miR-206 in keeping with the physiologic requirements may be more rational. Following transfection with miR-206 mimics in colon cancer cells, the mRNA and protein levels of *NOTCH3* were all downregulated. The same phenomenon has also been observed in HeLa (19) and HepG2 (34) cells. This finding supports the hypothesis that miRNAs are involved in gene regulation via post-transcriptional silencing on its targets and interfering with the transcription of target genes in an indirect manner. Initially, studies on miR-206 mostly focused in muscle tissue, which was due to the high tissue-specificity of miR-206 screened in high-throughput analyses (6). Occasionally, a significant expression of miR-206 was detected in normal murine skin (24,35) and HPV8-mediated skin tumors (36). Since the first evidence for the post-transcriptional regulation of ESR1 by miR-206 in MCF-7 breast cancer cells, miR-206 has been denoted as a tumor suppressor that is downregulated in many types of cancer, and a number of target genes, including oncogenes and tumor-suppressor genes, have been identified (37). Our results confirmed the repressive effect of miR-206 on *NOTCH3* expression at the mRNA and protein levels in CRC, which also suggests that miR-206 coordinates molecular networks in cancer.

Overexpressed miR-206 has been shown to attenuate colon cancer cell proliferation and migration *in vitro*. Such inhibitory effects of miR-206 are evident in other cancer models in which growth-associated targets, such as *CCNC* (15), *CCND1* (15), *CCND2* (14), *CDC42* (38), *CDK4* (15), *MET* (18), and *VEGF* (11), have been identified. The increase in cell number in the G_0/G_1 phase caused by miR-206 mimic transfection suggests that cyclin genes are involved in the regulatory networks of miR-206, and probably account for the downregulation of *NOTCH3* at the mRNA level. Therefore, underexpression of miR-206 in CRC may contribute to oncogenesis by dysregulating the cell-cycle drivers.

In contrast to Notch1, Notch2 and Notch4, Notch3 does not appear to be essential for embryonic develop-

ment as Notch3-null mice are viable and fertile, but have impaired maturation of vascular smooth muscle cells (39). NOTCH3 activation also protects against apoptosis through CBF1/RBP-Jκ independently, but cross-talks to the ERK/MAPK (40) or PI3-kinase/AKT (41) pathway, which emphasizes its indispensable role in maintaining cell viability. Thus, the downregulation of NOTCH3 following miR-206 mimic transfection increases apoptosis and caspase-3 content. Furthermore, MMP-2 and MMP-9, are crucial in tumor invasion and metastasis because of specificity for type IV collagen (the principal component of the basement membrane) (42), have been shown to be regulated by NOTCH3 via the ERK1/2 pathway, and strongly correlate with hepatocellular carcinoma metastasis (33). The invasion and migration of MDA-MB-231 breast cancer cells *in vitro* were inhibited with the downregulation of MMP-9 via miR-206 targeting *CDC42* (38). Similarly, *CDH2* (N-cadherin), mediating cell-cell interaction to prevent cell apoptosis by activating the PI3-kinase/AKT pathway (43), was downregulated following miR-206 mimic transfection in the current study. CDH2 was upregulated in dedifferentiated, invasive prostate carcinomas (44) and has been reported to participate in TNF-α-induced EMT in CRC cells (45). The levels of expression of *JAG1*, *HEY1*, and *CDH2* mRNA were higher in SW620 than SW480 cells, which supports the metastatic property of SW620 compared to its primary strain (SW480). Nevertheless, the upregulation of miR-206-induced tumor suppressive effects was similar in the 2 cell lines, suggesting miR-206 plays a fundamental role in the tumorigenesis of CRC involving multiple signaling pathways.

Consistent with previous reports, our results support the hypothesis that expressed miR-206 can decrease cell proliferation and migration, block the cell cycle, and activate apoptosis in CRC cells. The tumor suppressive capacity of miR-206 has a similar effect on CRC cells with different metastatic potential and may be explained by its direct NOTCH3 signaling inhibition and indirect cross-talk with other signaling pathways involving CDH2 and MMP-9. These results emphasize the potential therapeutic strategy for CRC by rescuing miR-206, which is downregulated in CRC. Future studies may continue to evaluate the effects of miR-206 on tumor growth *in vivo*, and to understand how it affects the pathogenesis of CRC, which may reveal feasible therapies for this disease.

Acknowledgements

The authors thank Dr Yuan Mu (Department of Clinical Laboratory, Nanjing Children's Hospital, Nanjing Medical University) for the technical assistance and helpful discussions.

References

1. Jemal A, Bray F, Center MM, Ferlay J, Ward E and Forman D: Global cancer statistics. CA Cancer J Clin 61: 69-90, 2011.
2. DeSantis CE, Lin CC, Mariotto AB, *et al*: Cancer treatment and survivorship statistics, 2014. CA Cancer J Clin 64: 252-271, 2014.
3. Eccles SA and Welch DR: Metastasis: recent discoveries and novel treatment strategies. Lancet 369: 1742-1757, 2007.
4. Hanahan D and Weinberg RA: Hallmarks of cancer: the next generation. Cell 144: 646-674, 2011.
5. Lee YS and Dutta A: MicroRNAs in cancer. Annu Rev Pathol 4: 199-227, 2009.
6. McCarthy JJ: MicroRNA-206: the skeletal muscle-specific myomiR. Biochim Biophys Acta 1779: 682-691, 2008.
7. Kondo N, Toyama T, Sugiura H, Fujii Y and Yamashita H: miR-206 Expression is down-regulated in estrogen receptor alpha-positive human breast cancer. Cancer Res 68: 5004-5008, 2008.
8. Taulli R, Bersani F, Foglizzo V, *et al*: The muscle-specific microRNA miR-206 blocks human rhabdomyosarcoma growth in xenotransplanted mice by promoting myogenic differentiation. J Clin Invest 119: 2366-2378, 2009.
9. Zhou L, Chen J, Li Z, *et al*: Integrated profiling of microRNAs and mRNAs: microRNAs located on Xq27.3 associate with clear cell renal cell carcinoma. PLoS One 5: e15224, 2010.
10. Wang X, Ling C, Bai Y and Zhao J: MicroRNA-206 is associated with invasion and metastasis of lung cancer. Anat Rec 294: 88-92, 2011.
11. Zhang T, Liu M, Wang C, Lin C, Sun Y and Jin D: Down-regulation of MiR-206 promotes proliferation and invasion of laryngeal cancer by regulating VEGF expression. Anticancer Res 31: 3859-3863, 2011.
12. Chen X, Yan Q, Li S, *et al*: Expression of the tumor suppressor miR-206 is associated with cellular proliferative inhibition and impairs invasion in ERα-positive endometrioid adenocarcinoma. Cancer Lett 314: 41-53, 2012.
13. Vickers MM, Bar J, Gorn-Hondermann I, *et al*: Stage-dependent differential expression of microRNAs in colorectal cancer: potential role as markers of metastatic disease. Clin Exp Metastasis 29: 123-132, 2012.
14. Zhang L, Liu X, Jin H, *et al*: miR-206 inhibits gastric cancer proliferation in part by repressing cyclinD2. Cancer Lett 332: 94-101, 2013.
15. Georgantas RW III, Streicher K, Luo X, *et al*: MicroRNA-206 induces G1 arrest in melanoma by inhibition of CDK4 and Cyclin D. Pigment Cell Melanoma Res 27: 275-286, 2014.
16. Missiaglia E, Shepherd CJ, Patel S, *et al*: MicroRNA-206 expression levels correlate with clinical behaviour of rhabdomyosarcomas. Br J Cancer 102: 1769-1777, 2010.
17. Adams BD, Furneaux H and White BA: The micro-ribonucleic acid (miRNA) miR-206 targets the human estrogen receptor-alpha (ERalpha) and represses ERalpha messenger RNA and protein expression in breast cancer cell lines. Mol Endocrinol 21: 1132-1147, 2007.
18. Yan D, Dong Xda E, Chen X, *et al*: MicroRNA-1/206 targets c-Met and inhibits rhabdomyosarcoma development. J Biol Chem 284: 29596-29604, 2009.
19. Song G, Zhang Y and Wang L: MicroRNA-206 targets notch3, activates apoptosis, and inhibits tumor cell migration and focus formation. J Biol Chem 284: 31921-31927, 2009.
20. Lardelli M, Dahlstrand J and Lendahl U: The novel Notch homologue mouse Notch 3 lacks specific epidermal growth factor-repeats and is expressed in proliferating neuroepithelium. Mech Dev 46: 123-136, 1994.
21. Serafin V, Persano L, Moserle L, *et al*: Notch3 signalling promotes tumour growth in colorectal cancer. J Pathol 224: 448-460, 2011.
22. Gagan J, Dey BK, Layer R, Yan Z and Dutta A: Notch3 and Mef2c proteins are mutually antagonistic via Mkp1 protein and miR-1/206 microRNAs in differentiating myoblasts. J Biol Chem 287: 40360-40370, 2012.
23. Wang WX, Wilfred BR, Baldwin DA, *et al*: Focus on RNA isolation: obtaining RNA for microRNA (miRNA) expression profiling analyses of neural tissue. Biochim Biophys Acta 1779: 749-757, 2008.
24. Mu Y, Zhou H, Li W, Hu L and Zhang Y: Evaluation of RNA quality in fixed and unembedded mouse embryos by different methods. Exp Mol Pathol 95: 206-212, 2013.
25. Livak KJ and Schmittgen TD: Analysis of relative gene expression data using real-time quantitative PCR and the 2(-Delta Delta C(T)) method. Methods 25: 402-408, 2001.
26. Guo R, Wu Q, Liu F and Wang Y: Description of the CD133+ subpopulation of the human ovarian cancer cell line OVCAR3. Oncol Rep 25: 141-146, 2011.
27. Tavazoie SF, Alarcon C, Oskarsson T, *et al*: Endogenous human microRNAs that suppress breast cancer metastasis. Nature 451: 147-152, 2008.
28. Bandres E, Cubedo E, Agirre X, *et al*: Identification by Real-time PCR of 13 mature microRNAs differentially expressed in colorectal cancer and non-tumoral tissues. Mol Cancer 5: 29, 2006.
29. Cummins JM, He Y, Leary RJ, *et al*: The colorectal microRNAome. Proc Natl Acad Sci USA 103: 3687-3692, 2006.
30. Monzo M, Navarro A, Bandres E, *et al*: Overlapping expression of microRNAs in human embryonic colon and colorectal cancer. Cell Res 18: 823-833, 2008.

31. Ozawa T, Kazama S, Akiyoshi T, *et al*: Nuclear Notch3 expression is associated with tumor recurrence in patients with stage II and III colorectal cancer. Ann Surg Oncol 21: 2650-2658, 2014.
32. Lee SH, Jeong EG and Yoo NJ: Mutational analysis of NOTCH1, 2, 3 and 4 genes in common solid cancers and acute leukemias. APMIS 115: 1357-1363, 2007.
33. Zhou L, Zhang N, Song W, *et al*: The significance of Notch1 compared with Notch3 in high metastasis and poor overall survival in hepatocellular carcinoma. PLoS One 8: e57382, 2013.
34. Liu W, Xu C, Wan H, *et al*: MicroRNA-206 overexpression promotes apoptosis, induces cell cycle arrest and inhibits the migration of human hepatocellular carcinoma HepG2 cells. Int J Mol Med 34: 420-428, 2014.
35. Anderson C, Catoe H and Werner R: MIR-206 regulates connexin43 expression during skeletal muscle development. Nucleic Acids Res 34: 5863-5871, 2006.
36. Hufbauer M, Lazic D, Reinartz M, Akgul B, Pfister H and Weissenborn SJ: Skin tumor formation in human papillomavirus 8 transgenic mice is associated with a deregulation of oncogenic miRNAs and their tumor suppressive targets. J Dermatol Sci 64: 7-15, 2011.
37. Nohata N, Hanazawa T, Enokida H and Seki N: microRNA-1/133a and microRNA-206/133b clusters: dysregulation and functional roles in human cancers. Oncotarget 3: 9-21, 2012.
38. Liu H, Cao YD, Ye WX and Sun YY: Effect of microRNA-206 on cytoskeleton remodelling by downregulating Cdc42 in MDA-MB-231 cells. Tumori 96: 751-755, 2010.
39. Domenga V, Fardoux P, Lacombe P, *et al*: Notch3 is required for arterial identity and maturation of vascular smooth muscle cells. Genes Dev 18: 2730-2735, 2004.
40. Wang W, Prince CZ, Mou Y and Pollman MJ: Notch3 signaling in vascular smooth muscle cells induces c-FLIP expression via ERK/MAPK activation. Resistance to Fas ligand-induced apoptosis. J Biol Chem 277: 21723-21729, 2002.
41. Wang T, Holt CM, Xu C, *et al*: Notch3 activation modulates cell growth behaviour and cross-talk to Wnt/TCF signalling pathway. Cell Signal 19: 2458-2467, 2007.
42. Zeng ZS, Cohen AM and Guillem JG: Loss of basement membrane type IV collagen is associated with increased expression of metalloproteinases 2 and 9 (MMP-2 and MMP-9) during human colorectal tumorigenesis. Carcinogenesis 20: 749-755, 1999.
43. Tran NL, Adams DG, Vaillancourt RR and Heimark RL: Signal transduction from N-cadherin increases Bcl-2. Regulation of the phosphatidylinositol 3-kinase/Akt pathway by homophilic adhesion and actin cytoskeletal organization. J Biol Chem 277: 32905-32914, 2002.
44. Tran NL, Nagle RB, Cress AE and Heimark RL: N-Cadherin expression in human prostate carcinoma cell lines. An epithelial-mesenchymal transformation mediating adhesion with stromal cells. Am J Pathol 155: 787-798, 1999.
45. Wang H, Wang HS, Zhou BH, *et al*: Epithelial-mesenchymal transition (EMT) induced by TNF-α requires AKT/GSK-3β-mediated stabilization of snail in colorectal cancer. PLoS One 8: e56664, 2013.
46. Tang F, Hajkova P, Barton SC, *et al*: MicroRNA expression profiling of single whole embryonic stem cells. Nucleic Acids Res 34: e9, 2006.